ELSEVIER

International Journal of Mass Spectrometry 214 (2002) 315–326

International Journal of Mass Spectrometry

www.elsevier.com/locate/ijms

Methane elimination from ionized 1-butene

Charles E. Hudson, David J. McAdoo*

Marine Biomedical Institute, University of Texas Medical Branch, 301 University Boulevard, Galveston, TX 77555-1043, USA

Received 10 September 2001; accepted 10 December 2001

Abstract

The elimination of methane from the 1-butene cation is characterized by B3LYP/6-31G(d) and ab initio theories. This reaction effectively occurs in two steps (1) C–C bond cleavage with migration of methyl to the bond between the second carbon and the hydrogen on that carbon, and (2) transfer of that H from allyl to methyl. This pathway differs from previously characterized alkane eliminations by radical cations in that both C–H distances in C···H···C are short around the point where H is half transferred, and the associated angle is substantially bent. Also, the charge is delocalized over both fragments during the course of the reaction, giving the migrating methyl considerable cationic character. The net unpaired spin is almost completely on the allyl carbons, so the methyl has almost negligible radical character. The observed electron distribution is attributed to hybridization due to the similarity in energies of CH_2=C=$CH_2^{\bullet+} + CH_3^{\bullet}$ and CH_2=C=$CH_2 + CH_3^+$, the species the H is transferred between. Overlap population analysis reveals substantial bonding not only between the transferring H and the carbons it bridges, but also between the methyl carbon and the middle allyl carbon. In previously studied alkane eliminations from radical cations in the gas phase, H-transfer occurs with the C, H and C involved being close to "in line," in contrast to the present H-abstraction essentially by attack by methyl on a C–H bond. (Int J Mass Spectrom 214 (2002) 315–326) © 2002 Elsevier Science B.V. All rights reserved.

Keywords: $C_4H_8^+$; Ab initio; Ion–neutral complex; Alkane elimination

1. Introduction

The dissociations of $C_4H_8^{\bullet+}$ ions have been extensively investigated in developing rate theories for unimolecular dissociations [1–4]. The transition state for methane elimination from $C_4H_8^{\bullet+}$ was assumed to involve 1,3-H transfers concerted with C–C bond rupture (Scheme 1). A tight transition state was required to obtain RRKM rates for methane elimination from the 1-butene ion comparable to experimental ones [4].

However, associated efforts to locate a transition state for methane elimination from the 1-butene ion (**1**) by ab initio means were unsuccessful, so the exact nature of that transition state is unknown, despite its being for an important model reaction. Alkane eliminations from radical cations in the gas phase generally take place through alkyl radical-ion complexes in which bond-breaking and H-transfer are effectively separate steps [5–7]. Alkane [8–12], alcohol [13,14], ketone [13,15,16], amine [13,17], ether [18–22] and enolate [23,24] ions all eliminate alkanes. Facile cleavages that occur beta to the double bonds of olefin ions [25] (Scheme 2) might generate ion–neutral complexes akin to those that mediate other alkane eliminations [5–7], suggesting that methane elimination from **1** is complex-mediated (Scheme 2).

In light of the importance of the $C_4H_8^{\bullet+}$ model system and of the associated mechanistic uncertainties,

* Corresponding author. E-mail: djmcadoo@utmb.edu

1387-3806/02/$20.00
PII S1387-3806(02)00524-9

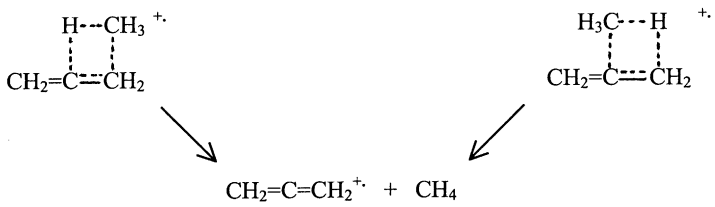

Scheme 1.

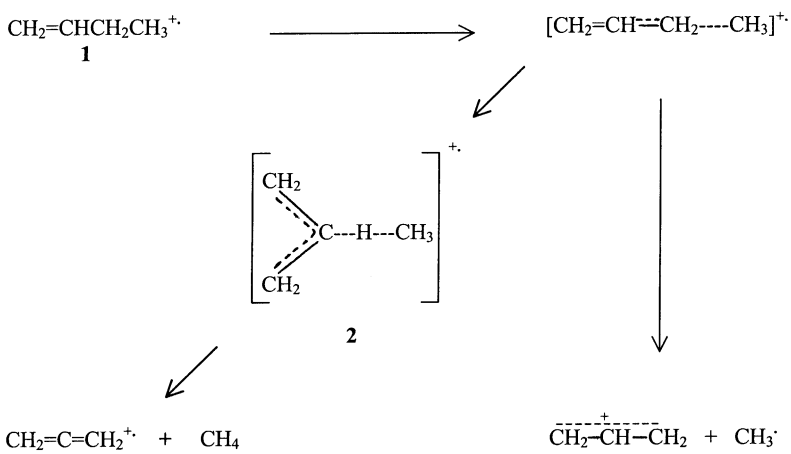

Scheme 2.

we undertook an ab initio study of the dissociations of **1** with emphasis on elucidating the pathway for methane elimination. This starting point was selected because methane elimination from $C_4H_8^{\bullet+}$ ions most likely starts from **1** rather than from another isomer [4]. We found that that pathway goes through a very unusual methyl–allyl complex that has its charge spread substantially over both partners, quite different from previously described simple ion–dipole and ion-induced dipole complexes.

2. Theory

All computations were performed using the Gaussian 94 and Gaussian 98W suites of programs [26,27] on Cobra Carrera Alpha and Dell Dimension 4100 computers, respectively. Hybrid B3LYP/6-31G(d) theory was used for initial location of stationary points followed by refined characterization at higher levels of ab initio theory. Transition states were located as optima with a single imaginary frequency. Intrinsic reaction coordinate (IRC) calculations [28,29] at the B3LYP/6-31G(d) level of theory were used in efforts to relate transition states to the stable minima they connect. Zero point energies were obtained by B3LYP/6-31G(d) theory because QCI theory does not give analytical force constants. Zero point energies were corrected by multiplying those derived from frequencies produced by B3LYP/6-31G(d) theory by the scaling factor 0.9806 [30].

3. Results and discussion

3.1. The $C_4H_8^{\bullet+}$ potential surface

The compound **1**, several transition states and an energy minimum at an allyl–methyl complex (**2**) were located by theory on the pathway to methane elimination

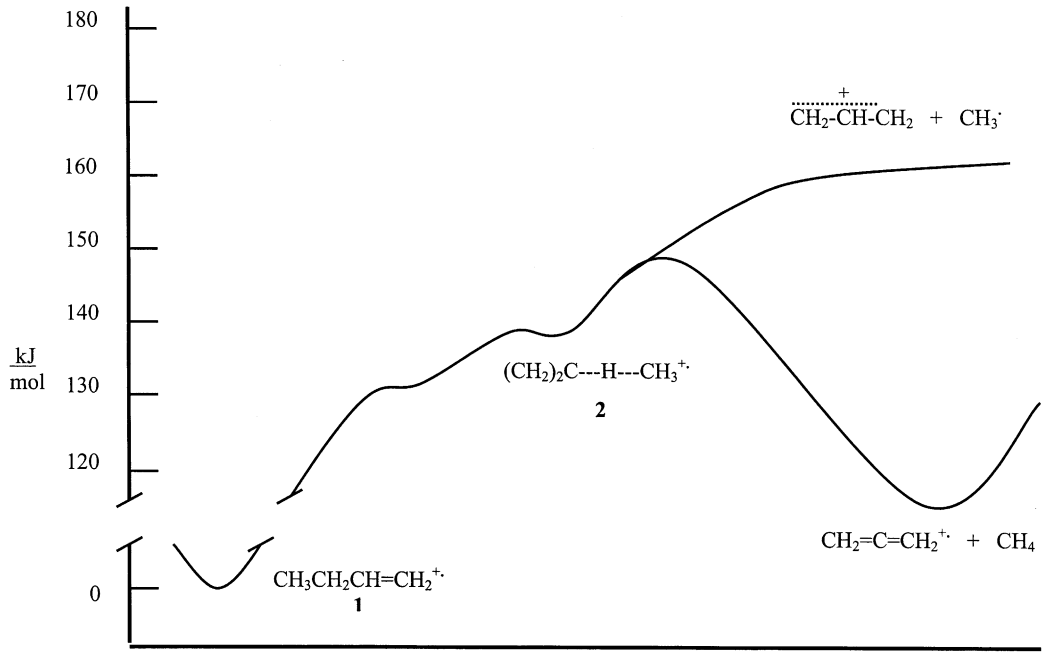

Fig. 1. Potential surface for the decompositions of the 1-butene ion based on energies obtained at the QCISD(T)/6-311G(d,p)// QCISD/6-31G(d) level of theory.

from **1**. These correspond to stationary points expected for the reactions in Scheme 2. Energies of the stationary points obtained at several levels of theory are given in Table 1, and a potential diagram depicting the relevant region of the $C_4H_8^{\bullet+}$ potential surface obtained by QCISD(T)/6-311G(d,p)//QCISD/6-31G(d) theory is given in Fig. 1. The relative theoretical energies are similar to relative experimental ones where comparisons can be made, the relative theoretical values being within 10 kJ mol^{-1} of the corresponding relative experimental values (Table 2). At the stable minimum **2**, a methyl is joined to the middle carbon (C_2) of allene and the hydrogen atom (H^t) on that carbon. Even though several transition states were located that may occur between **1** and **2**, only one, designated TS(**1** → **2**), was chosen for detailed characterization. Although TS(**1** → **2**) is higher in energy than **2** without zero point energy corrections, incorporating zero point energies into the results lowers the energy of TS(**1** → **2**) below that of **2**, so **2** may not be an energy minimum. Two maxima appear between **1** and **2** in Fig. 1 because TS(**1** → **2**) has only one imaginary frequency and at the same time is lower in energy than **2**, which is an apparent energy minimum. Although **2** may not be an energy minimum, we nonetheless present a theoretical description of **2** because it provides a convenient point to characterize on the reaction coordinate and because an ion–neutral complex need not be in a potential minimum [9,31,32]. The geometries, including pertinent bond angles and lengths, found for **1** and stationary points along the reaction coordinate are given in Figs. 2–5.

3.2. $[(CH_2{=})_2C\cdots H^t\cdots CH_3]^{\bullet+}$ (2)

As already noted, **2** corresponds to a methyl joined to allene through the hydrogen on the middle carbon (C_2) of allene and by direct interactions with that carbon (Fig. 3). The methyl carbon in **2** is close to the plane of the other three carbons. The C–H^t–C bond angle in **2** is 100.8°, far from the approximate linearity typical of X–H–X configurations in previously

Table 1
Energies (Hartrees) of stationary points related to the $C_4H_8^{\bullet+}$ potential surface

	B3LYP/6-31G(d)[a]	QCISD/6-31G(d)[a]	QCISD/6-311G(d,p)// QCISD/6-31G(d)	QCISD(T)/6-311G(d,p)// QCISD/6-31G(d)	ZPE[b] (kJ mol^{-1})	ΔE[c] species (kJ mol^{-1})
CH_2=$CHCH_2CH_3^{\bullet+}$ (**1**)	−156.883548	−156.338755	−156.447133	−156.466171	271.5	0
TS(**1** → $\bar{C}H_2\bar{C}H\bar{C}H_2^+ + CH_3^{\bullet}$)	−156.823660[d]				257.0	
TS(**2** → $\bar{C}H_2\bar{C}H\bar{C}H_2^+ + CH_3^{\bullet}$)	−156.814408[d]				254.7	
$\bar{C}H_2\bar{C}H\bar{C}H_2^+$	−116.972219	−116.579154	−116.648589	−116.666123	176.9	
$CH_3^{\bullet}$	−39.838292	−39.689122	−39.729163	−39.732301	76.8	
$\bar{C}H_2\bar{C}H\bar{C}H_2^+ + CH_3^{\bullet}$	−156.810511	−156.268276	−156.377752	−156.398424	253.7	160.1
$(CH_2)_2C\cdots H\cdots CH_3^{\bullet+}$ (**2**)	−156.821341	−156.273057	−156.387687	−156.410016	261.5	137.4
TS(**1** → **2**)	−156.821175	−156.272724	−156.386953	−156.409412	254.7	132.2
TS(**2** → CH_2=C=$CH_2^{\bullet+} + CH_4$)	−156.820992	−156.269079	−156.382364	−156.405060	258.0	146.9
CH_2=C=$CH_2^{\bullet+}$	−116.315722	−115.931995	−115.992087	−116.008277	136.6	
CH_4	−40.518389	−40.353370	−40.401641	−40.405948	116.4	
CH_2=C=$CH_2^{\bullet+} + CH_4$	−156.834111	−156.285365	−156.393728	−156.414225	253.0	117.9
CH_2=C=$CH_2^{\bullet+} + CH_3^{\bullet}$	−156.154014	−155.621117	−155.721250	−155.740578	213.4	0[e]
CH_3^+	−39.480388	−39.345965	−39.378981	−39.381142	81.5	
CH_2=C=CH_2	−116.657676	−116.268026	−116.337973	−116.356694	142.9	
CH_2=C=$CH_2 + CH_3^+$	−156.138064	−155.613991	−155.716954	−155.737836	224.4	18[e]

[a] Structure and energies obtained at the same level of theory.
[b] Obtained at the B3LYP/6-31G(d) level of theory.
[c] Derived from the results at the QCSID(T)/6-311G(d,p)//QCISD/6-31G(d) + ZPE level of theory.
[d] This transition state was not found at higher levels of theory.
[e] Values are relative to each other.

Table 2
Pertinent experimental heats of formation (kJ mol^{-1})

Species	ΔH_f[a]	Relative energy[b]
CH_2=$\underline{CH}\underline{CH_2}CH_3^{\bullet+}$	924	0
$\underline{CH_2}\underline{CH}CH_2^+$	945.6	
$CH_3^\bullet$	145.8	
$\underline{\underline{CH_2}}\,\underline{\underline{CH}}\underline{\underline{CH_2}}^+ + CH_3^\bullet$	1091.4	167
$\underline{\underline{CH_2}}\,\underline{\underline{CH}}\underline{\underline{CH_2}}^\bullet$	161	
CH_3^+	1093.3	
$\underline{\underline{CH_2}}\,\underline{\underline{CH}}\underline{\underline{CH_2}}^\bullet + CH_3^+$	1254	330
CH_4	−74.5	
CH_2=C=$CH_2^{\bullet+}$	1126	
CH_2=C=$CH_2^{\bullet+} + CH_4$	1051.5	128
CH_2=C=CH_2	191	
CH_2=C=$CH_2^{\bullet+} + CH_3^\bullet$	1271.8	
CH_2=C=$CH_2 + CH_3^+$	1284	

[a] [46].
[b] Relative to the 1-butene ion = 0.

described ion–neutral complexes [16,33–37]. H^t is far out of the plane of the carbons in **2**. In **1**, the carbons and the hydrogens on C_1 and C_2 are all in a plane, so there is substantial movement of H^t during transformation from **1** to **2**. The two C–H^t bonds to H^t in **2** are similar in length (1.216 Å to C_2 and 1.268 Å to C_{Me}), that is, H^t is close to halfway between the two carbons in this complex. These distances are longer than normal C–H lengths (the C–H distances in the departing methyl in **2** are 1.086–1.096 Å), but much shorter than the longer of two C–H distances to the H being transferred in previously characterized ion–methyl complexes for [$CH_3^\bullet$ $CH_3CH^+CH_3$] 3.831 Å [9], [$CH_3^\bullet$ CH_3CO^+] 2.537 Å [16], [$CH_3^\bullet$ $C_2H_5^+$] 1.983 Å [11] and 2.657 Å in [$CH_3^\bullet$ CH_3CH=O^+CH_3] [20]. Excepting the complex containing $C_2H_5^+$ in which the hydrogen connecting the partners also bridges the ethyl carbons, the short C–H bonds to the connecting hydrogen in these complexes average 1.11 Å in length, i.e., are nearly normal. Its two short C–H^t distances distinguish **2** from previously described cation-alkyl radical complexes. The methyl C is almost equidistant from the end carbons of the C_3 fragment, 2.737 and 2.757 Å. We regard **2** as a complex because the lengthened and essentially equal C–C distances from the methyl to C_1 and C_3 at TS(**1** → **2**) demonstrate

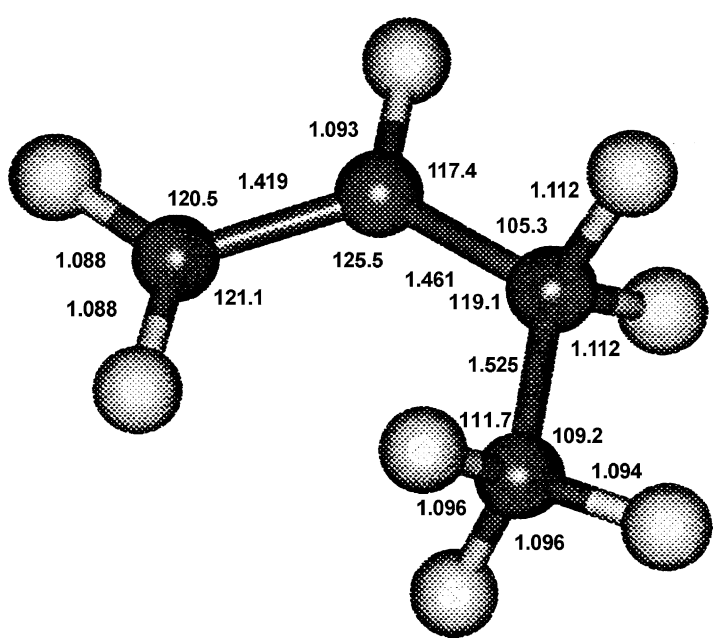

Fig. 2. Structure of the 1-butene ion at the QCISD/6-31G(d) level of theory. Distances are in angstroms (Å) and angles are in degrees (°).

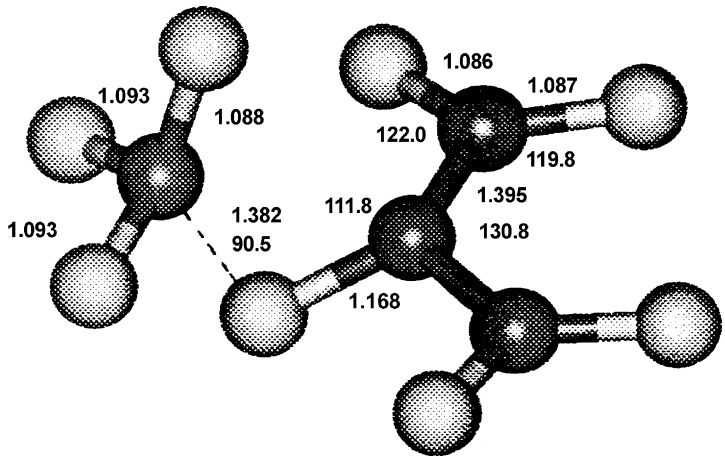

Fig. 3. Structure of TS(**1** → **2**) at the QCISD/6-31G(d) level of theory.

that the C–C bond in **1** to the moving methyl is completely broken before **2** is reached. However, **2** is quite different from the ion-induced dipole bound complexes that have been described previously [6,7,39].

Analysis of the vibrational motions of **2** revealed three modes involving substantial motion of H^t toward the approximate plane of the four carbon atoms. In one with a frequency of 166 cm^{-1}, the C_2 and methyl carbons moved apart as H^t moved toward a line between them. In the others with frequencies of 1776 and 2025 cm^{-1}, there was little motion of the carbons as H^t moved toward their connecting axis. In one of these, H^t also had substantial simultaneous motion toward C_2, and in the other it moved toward the methyl carbon. Given that the lowest frequency motion of H^t toward the C–C axis was accompanied by movement of the carbons away from each other, near linearity

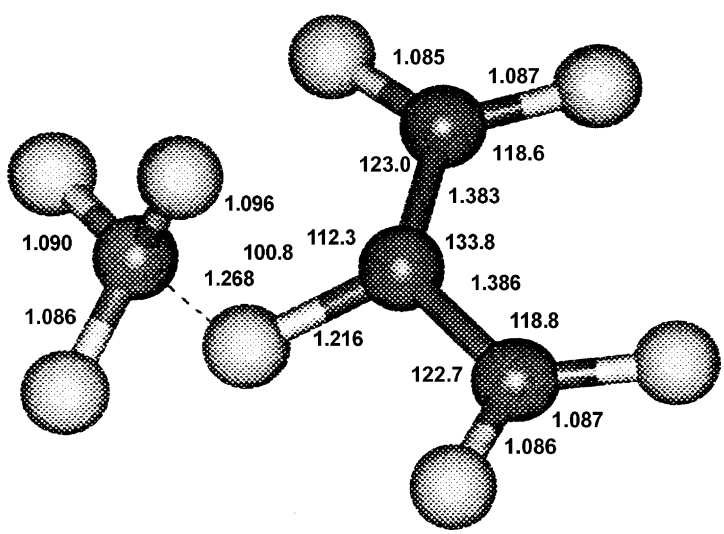

Fig. 4. Structure of $[(CH_2)_2C\cdots H\cdots CH_3]^{\bullet+}$ at the QCISD/6-31G(d) level of theory.

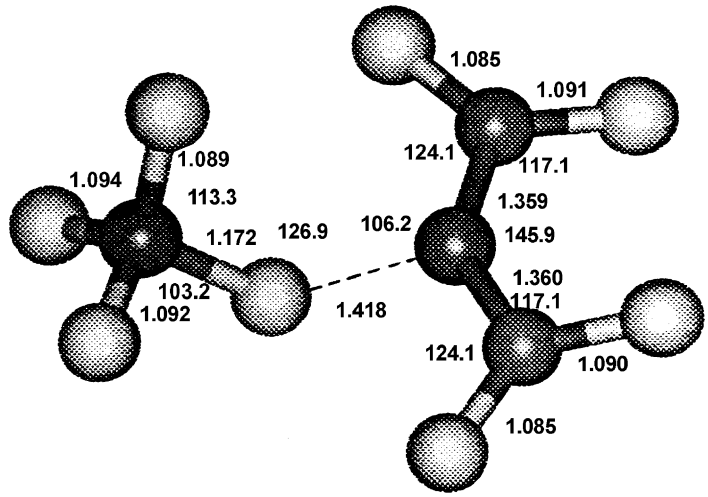

Fig. 5. Structure of TS(**2** → $C_3H_4^{\bullet+}$ + CH_4) at the QCISD/6-31G(d) level of theory.

of C–H^t–C appears to require a longer C–C distance than that in **2**; that is, the C_2–C_{Me} attractions force H^t out of the plane of the carbons.

Charge and spin distributions on all four carbons and on H^t based on Mulliken population analysis at stationary points are given in Table 3. Charge distributions are given as sums of those on carbon and its attached hydrogens to reduce the arbitrariness of the division of charge densities between atoms that this procedure employs [38]. These distributions further differentiate **2** from previously described ion-alkyl radical complexes in that approximately half a unit charge is assigned to the methyl, and the net spin is largely dispersed over the C–C–C moiety at **2**. Previously characterized complexes containing methyl partners have according to theory the unpaired spin largely assigned to the methyl and the charge to the incipient ion (in [$CH_3^{\bullet}$ $CH_3CH^+CH_3$] the total of the net atomic charges in the propyl moiety is +0.907, and the total spin density on the methyl radical is 0.905 [9]; in [$CH_3^{\bullet}$ $C_2H_5^+$] the charge on ethyl is +0.985 and the spin density on methyl is 0.970 [11], in [$CH_3^{\bullet}$ CH_3O^+=$CHCH_3$] the net charge is +0.965 on the ion and the total spin density on the methyl is

Table 3
Charge and spin locations[a] at stationary points on the $C_4H_8^{\bullet+}$ potential surface

	C_1	C_2	C_3	C_{Me}	H^t
Charge[b]					
TS(**1** → **2**)	0.239	−0.014	0.239	0.537	0.408
$(CH_2)_2C\cdots H\cdots CH_3^{\bullet+}$	0.219	0.060	0.218	0.502	0.374
TS(**2** → CH_2=C=$CH_2^{\bullet+}$ + CH_4)	0.255	0.200	0.247	0.297	0.226
Spin[c]					
TS(**1** → **2**)	0.743	−0.268	0.743	0.036	
$(CH_2)_2C\cdots H\cdots CH_3^{\bullet+}$	0.732	−0.296	0.753	−0.021	
TS(**2** → CH_2=C=$CH_2^{\bullet+}$ + CH_4)	0.640	−0.226	0.670	0.051	

[a] Values were obtained at the QCISD/6-311G(d)//QCISD/6-31G(d) level of theory using the QCI density.
[b] Charges were obtained by summing Mulliken charge densities on carbons and hydrogens attached to them. The charge on H^t was divided evenly between C_2 and CMe in each case.
[c] Spins are the net spins on each carbon obtained by Mulliken population analysis.

Table 4
Overlap populations[a] between the transferring H and the carbons it is moving between

	H^t–C_2	H^t–C_{Me}	C_{Me}–C_2	C–C[b]	C–H[c]
TS(**1** → **2**)	0.438	0.102	0.224	0.708	0.712
2	0.223	0.341	0.222	0.748	0.708
TS(**2** → $C_3H_4^{+\bullet}$ + CH_4)	0.190	0.436	0.085	0.833	0.705

[a] Sums of the two values obtained at the QCISD/6-31G(d) level of theory.
[b] Average of values for the two C–C bonds.
[c] Average of values for all C–H bonds except those to H^t.

0.965 [20]). The electron delocalization over both partners prevents **2** from being an "orbiting pair," in contrast to electrostatically-bound ion–neutral complexes that have hitherto been described [32]. A fixed structure is expected in complexes in which the partners are held together by a hydrogen bond [31,39].

Overlap populations (Table 4) show the existence of substantial covalent bonding of H^t to both the methyl carbon and C_2 in **2**. At the QCISD/6-31G(d) level of theory the H^t–C_2 overlap is 0.223 and the H^t–C_{Me} overlap is 0.341. An overlap of 0.222 between C_{Me} and C_2 demonstrates that there is also significant bonding between those carbons. This and the overlap between C_{Me} and H^t demonstrates that C_{Me} essentially methylates the C_2–H^t bond in **2**. The average overlap for the remaining C–H bonds in **2** is 0.708, providing a measure of overlap for a normal C–H bond. Interactions between C_2, C_{Me} and H^t are substantial because these overlaps are much greater than those between non-bonded atoms. The latter are mostly small negative numbers, and the most positive overlap for a non-bonding interaction in **2** is 0.0017. The C···H···C geometry of **2** likely derives from the methyl interacting with C_2 and H^t simultaneously.

We attribute the delocalization of the charge and spin during H transfer to hybridization arising from the similarity in energy of CH_2=C=$CH_2^{\bullet+}$ + $CH_3^{\bullet}$ vs. CH_2=C=CH_2 + CH_3^+ (Table 2). Based on experimental values (Table 2), $CH_3^{\bullet}$ + CH_2=C=$CH_2^{\bullet+}$ (1271.8 kJ mol^{-1}, Table 2) and CH_3^+ + CH_2=C=CH_2 (1284.3 kJ mol^{-1}) differ in stability by only 12.5 kJ mol^{-1}. Neglecting ZPE corrections, QCISD(T)/6-311G(d,p)//QCISD/6-31G(d) theory, the highest level we applied, places $CH_3^{\bullet}$ + CH_2=C=$CH_2^{\bullet+}$ 7 kJ mol^{-1} CH_3^+ + CH_2=C=CH_2. ZPE corrections increase this difference to 18 kJ mol^{-1}, a value in quite good agreement with the corresponding difference of 12.5 kJ mol^{-1} between the experimental values. Zero point energies would not influence the theoretical description of the geometry of **2**. When H^t is about half transferred, the charge would have a comparable tendency to be associated with either C_3H_4 or CH_3, resulting in its distribution over both. It has been suggested that when two partners in an anion–neutral complex have similar electron affinities, the complex becomes a hybrid of the species with the charge located on each partner [40].

The covalent interactions of H^t with both C_{Me} and C_2 likely makes the C–H^t bond distances in **2** much shorter than the longer X–H distances already noted in previously characterized complexes. This indicates considerable covalent interaction in the C–H^t interactions in **2**. Based on van der Waals radii of 1.06 Å for H and 1.53 Å for C [41], simple contact between H and C would give a C–H distance of 2.59 Å, much longer than the C···H^t···C, C–H distances in **2**. In other ion–neutral complexes, the long C–H distances found by ab initio methods are similar to the sum of the van der Waals radii of the atoms involved. This suggests that the most stable configuration of partners in a typical ion–neutral complex has the partners just "touching" each other.

The energy required to dissociate **2** to $CH_3^{\bullet}$ + $C_3H_5^+$ at the highest level of theory that we applied is 22.7 kJ mol^{-1}. This is comparable to the binding energies in other methyl-containing ion–neutral complexes: [$CH_3^{\bullet}$ CH_3CO^+] 20.5 kJ mol^{-1} [16], [$CH_3^{\bullet}$ $C_2H_5^+$] 39 kJ mol^{-1} [11], [$CH_3^{\bullet}$ CH_3CH=O^+CH_3]

Table 5
Characteristics of structures[a] near the pathway to methane elimination from the 1-butene cation

	C_{Me}–C_3	C_{Me}–C_1	C_2–H^t	C_{Me}–C_2	C_{Me}–H^t	ΔE
1	1.524	3.061	1.091	2.588	3.558	0
TS(**1**)	2.473	2.343	1.094	1.734	2.146	112.0
TS(**2**)	2.602	2.594	1.157	1.607	2.115	115.7
TS(**1** → **2**)	2.735	2.735	1.194	1.893	1.330	163.7
2	2.812	2.812	1.251	2.018	1.249	163.3
TS(**2** → $C_3H_4^{+\bullet}$ + CH_4)	2.913	2.926	1.321	2.182	1.210	164.2

[a] Obtained by B3LYP/6-31G(d) theory.

11.7 kJ mol^{-1} [20], [$CH_3^{\bullet}$ $CH_3CH^+CH_3$] 13.0 kJ mol^{-1} [9].

3.3. Transition states

Attempts to connect transition states to stable minima using IRC methods yielded a complex picture of the potential surface around **2**. Because of this complexity, the IRC calculations typically halted after going short distances. At least five transition states were located near **2** by IRC methods. To characterize a pathway to methane elimination, we ordered the stationary points located in terms of increasing C_2–H^t and decreasing C_{Me}–H^t distances (Table 5). In all pathways located starting from **2**, the methyl remained very near a plane of symmetry through C_2 over the distances we traced. In order to locate a pathway from **2** to **1**, the methyl had to be shifted slightly away from **2** toward **1**, so a continuous path from **2** to **1** was not actually located. A pathway that ended up at the 2-methylpropene ion was also located by an IRC calculation starting from TS(**1** → **2**) followed by ordinary optimization. The stationary points located around **2** superficially resemble a form of the methylcyclopropane ion that has a long bond between C_2 and C_3 [42] (C_1 and C_3 in our nomenclature for species around **2**). However, our structures can be distinguished from ionized methylcyclopropane isomers by C_1–C_3 distances of at least 2.52 Å in all species characterized here vs. published values of 1.49–1.81 Å for corresponding distances in ionized methylcyclopropane isomers [42]. We found a C_2–C_3 distance in the methylcyclopropane ion with a long bond between C_2 and C_3 of 1.84 Å by B3LYP/6-31G(d) theory. In addition, for species characterized here the CH_2 groups are nearly coplanar with the C_1–C_2–C_3 plane until twisting to an allene geometry starts to occur at TS(**2** → $C_3H_4^{\bullet+}$ + CH_4). The CH_2 are nearly perpendicular (within ±2.1°) to the ring in the methylcyclopropane cation with the long bond between the unsubstituted carbons by B3LYP/6-31G(d) theory.

At TS(**1** → **2**), the allyl group is bisected by a plane of symmetry that contains the methyl carbon, the migrating H and the middle carbon of the allyl group. As would be expected, H^t is closer to C_2 in TS(**1** → **2**) (1.168 Å from C_2 and 1.382 Å from C_{Me}) and closer to C_{Me} in TS(**2** → $C_3H_4^{\bullet+}$ + CH_4) (1.418 Å from C_2 and 1.172 Å from C_{Me}). Relative to **2**, the C–H^t–C angle is narrower in TS(**1** → **2**) (90.5°) and wider in the transition state for **2** → products (126.9°). Thus, the C–H^t–C angle opens steadily as H^t moves from the second carbon of the butene ion to methyl. The C–C–C angle also increases over the course of methane elimination (from 125.5° in **1** to 133.8° in **2** to 180° in the allene ion). The distances between the methyl C and the end carbons of the C_3 group in TS(**1** → **2**) are 2.683 and 2.684 Å. Thus, the initial C–C bond is completely broken by the time the system reaches TS(**1** → **2**). Therefore, like ion–neutral complex-mediated reactions [6,32,43], **1** eliminates methane in two steps, C–C bond breaking followed by H-transfer, rather than in a concerted process as assumed previously [4]. In **2** and the transition states, the methyl is interacting with the C_2–H^t bond. Thus, the methyl acquires H^t essentially by attacking the C–H bond

(**3**), in contrast to the pulling of H^t away by attack from the side of H^t opposite C_2 (**4**), as usually occurs in alkane eliminations [9,11,16,20]. Thus, there are at least three ways in which alkane eliminations can occur from cations in the gas phase, through an "orbiting" pair [6,7,31], by attack on a C–H bond as found here, and through a high energy, highly strained transition state [44]:

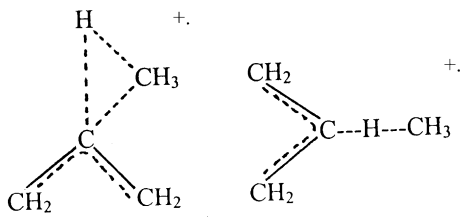

3 **4**

In TS(**1** → **2**), the summed overlap equals 0.438 for H^t–C_2 and 0.102 for H^t–C_{Me} at the QCISD/6-31G(d) level of theory (Table 4). Thus, at this point H^t is still strongly bound to the C it is leaving and weakly bound to the one it is approaching. In the transition state for methane elimination, the pattern is reversed (H^t–C_2 = 0.190, H^t–C_{Me} = 0.436). The overlap populations demonstrate that there is substantial covalent bonding between H^t and both associated carbons during the actual H-transfer. The C_{Me}–C_2 overlap is 0.224 in TS(**1** → **2**) and 0.085 in the transition state for methane elimination, so overlap between C_{Me} and C_2 diminishes steadily as H^t is transferred. In TS(**1** → **2**) the overlaps between C_{Me} and both C_1 and C_3 are small negative numbers, demonstrating that covalent bonding between C_{Me} and C_1 is completely broken off before TS(**1** → **2**) is reached, and therefore before the H-transfer to form methane is very far along. As in **2**, the methyl carries substantial positive charge that diminishes as H^t moves closer to C_{Me} (Table 3). The unpaired spin remains associated with the allene portion of the system throughout.

TS(**2** → $CH_4 + C_3H_4^{\bullet+}$) is 29 kJ mol^{-1} above the corresponding products, in reasonable agreement with the corresponding value of 22 kJ mol^{-1} estimated by Baer and coworkers [4] by fitting RRKM results to experimental rates of dissociation. At the highest level of theory we applied, the transition state energy for methane elimination was 13.2 kJ mol^{-1} below the threshold for dissociation to $C_3H_5^+ + CH_3^{\bullet}$, in the range of the 12–21 kJ mol^{-1} of such values for dissociation from ion-alkyl radical complexes [9,18,20].

Baer and coworkers found an entropy of activation of $-15.9\,J\,mol^{-1}\,K^{-1}$ at 1000 K for methane elimination from the butene ions [4] utilizing frequencies required to produce a good fit of RRKM results to their experimental data. We calculated a much smaller entropy difference of $-0.5\,J\,mol^{-1}\,K^{-1}$ between TS(**2** → $C_3H_4^{\bullet+} + CH_4$) and **1**, a value suggesting little tightening of that transition state. The present transition state is quite different in its nature from the concerted 1,3-H-shift that they assumed; among other differences, it is the methyl rather than the H that shifts. Our transition state may appear "looser" than they predicted because we considered the dissociation to occur only from **1**, whereas $C_4H_8^{\bullet+}$ is actually quite labile, rapidly interconverting among 1-butene, *cis*- and *trans*-2-butene, 2-methylpropene and methylcyclopropane ions relative to its rate of dissociation [45]. Taking the latter into consideration in determining the reactant entropy would increase the density of states for the reactant substantially relative to those employed in our calculation, thus making the entropy of activation much more negative, perhaps explaining the value obtained by Baer and coworkers [4].

We found a transition state for methyl loss from **1** at the B3LYP/6-31G(d) level of theory, but not at higher levels. Baer and coworkers were unable to find such a transition state by 3-21G theory. We did find a distinct transition state for the dissociation of the complex **2** to CH_2–CH–$CH_2^+ + CH_3^{\bullet}$ at the B3LYP/6-31G(d) level of theory. However, QCISD optimization starting from this B3LYP geometry gave the transition state for **2** → $CH_4 + C_3H_4^{\bullet+}$, so TS(**2** → $CH_3^{\bullet} + C_3H_5^+$) probably does not exist either. Thus, methyl may be lost from **1** along a pathway of continuously increasing energy until dissociation is complete without passing a saddle point. The absence of a conventional transition state for methyl loss is consistent with the earlier conclusions [2,4] that minimum entropy transition

states rather than saddle points control the rate of this reaction.

4. Summary

Previous work revealed alkane eliminations from ions in the gas phase through electrostatically bound ion–neutral pairs and through strained, high energy transition states. The characterization of **2** here reveals a new type of ion–neutral complex approximating a methyl cation interacting with a C–H bond. A parallel new mechanism for alkane elimination, hydrogen transfer by attack of a methyl cation on a C–H bond, is also revealed. A number of transition states appear to occur near **2**, suggesting a complex surface when CH_3 is essentially in the plane that bisects the C_3H_5 partner. Methyl loss from **1** probably occurs along a reaction coordinate monotonically increasing in energy, consistent with transition states located by the criterion of the point of minimum flux being rate controlling for that reaction.

Acknowledgements

We thank Debbie Pavlu for assistance in manuscript preparation.

References

[1] G.G. Meisels, G.M.L. Verboom, M.J. Weiss, T. Hsieh, J. Am. Chem. Soc. 101 (1979) 7189.
[2] W.J. Chesnavich, L. Bass, T. Su, M.T. Bowers, J. Chem. Phys. 74 (1981) 2228.
[3] M.T. Bowers, M.F. Jarrold, W. Wagner-Redeker, P.R. Kemper, L.M. Bass, Faraday Discuss. Chem. Soc. 75 (1983) 57.
[4] J.A. Booze, M. Schweinsberg, T. Baer, J. Chem. Phys. 99 (1993) 4441.
[5] C.E. Hudson, D.J. McAdoo, Int. J. Mass Spectrom. Ion Processes 59 (1984) 325.
[6] D.J. McAdoo, Mass Spectrom. Rev. 7 (1988) 363.
[7] D.J. McAdoo, R.D. Bowen, Eur. Mass Spectrom. 5 (1999) 389.
[8] J.F. Wendelboe, R.D. Bowen, D.H. Williams, J. Am. Chem. Soc. 103 (1981) 2333.
[9] S. Olivella, A. Solé, D.J. McAdoo, L.L. Griffin, J. Am. Chem. Soc. 116 (1994) 11078.
[10] J.C. Traeger, C.E. Hudson, D.J. McAdoo, J. Am. Soc. Mass Spectrom. 7 (1996) 73.
[11] S. Olivella, A. Solé, D.J. McAdoo, J. Am. Chem. Soc. 118 (1996) 9368.
[12] D.J. McAdoo, S. Olivella, A. Solé, J. Phys. Chem. A 102 (1998) 10798.
[13] S. Hammerum, K.F. Donchi, P.J. Derrick, Int. J. Mass Spectrom. Ion Phys. 47 (1983) 347.
[14] S. Hammerum, H.E. Audier, J. Chem. Soc., Chem. Commun. (1988) 860.
[15] J.C. Traeger, C.E. Hudson, D.J. McAdoo, J. Phys. Chem. 92 (1988) 1519.
[16] N. Heinrich, F. Louage, C. Lifshitz, H. Schwarz, J. Am. Chem. Soc. 110 (1988) 8183.
[17] P. Longevialle, Rap. Commun. Mass Spectrom. 9 (1995) 1189.
[18] D.J. McAdoo, J.C. Traeger, C.E. Hudson, L.L. Griffin, J. Phys. Chem. 92 (1988) 1524.
[19] D.J. McAdoo, C.E. Hudson, J.C. Traeger, A. Grose, L.L. Griffin, J. Am. Soc. Mass Spectrom. 2 (1991) 261.
[20] S. Olivella, A. Sole, D.J. McAdoo, L.L. Griffin, J. Am. Chem. Soc. 117 (1995) 2557.
[21] S. Hammerum, M.M. Hansen, H.E. Audier, Int. J. Mass Spectrom. Ion Processes 160 (1997) 183.
[22] R.D. Bowen, P. Clifford, J.T. Francis, J.K. Terlouw, Int. J. Mass Spectrom. Ion Processes 165/166 (1997) 155.
[23] R.N. Hayes, J.C. Sheldon, J.H. Bowie, Int. J. Mass Spectrom. Ion Processes 71 (1986) 233.
[24] J.H. Bowie, M.B. Stringer, G.J. Currie, J. Chem. Soc., Perkin Trans. II (1986) 1821.
[25] F.W. McLafferty, F. Turecek, Interpretation of Mass Spectra, University Science Books, Mill Valley, CA, 1993, p. 57, 230.
[26] M.J. Frisch, G.W. Trucks, H.B. Schlegel, P.M.W. Gill, B.G. Johnson, M.A. Robb, J.R. Cheeseman, T. Keith, G.A. Petersson, J.A. Montgomery, K. Raghavachari, M.A. Al-Laham, V.G. Zakrzewski, J.V. Ortiz, J.B. Foresman, J. Cioslowski, B.B. Stefanov, A. Nanayakkara, M. Challacombe, C.Y. Peng, P.Y. Ayala, W. Chen, M.W. Wong, J.L. Andres, E.S. Replogle, R. Gomperts, R.L. Martin, D.J. Fox, J.S. Binkley, D.J. Defrees, J. Baker, J.P. Stewart, M. Head-Gordon, C. Gonzalez, J.A. Pople, Gaussian 94 Revision E.2, Gaussian Inc., Pittsburgh, PA, 1995.
[27] M.J. Frisch, G.W. Trucks, H.B. Schlegel, G.E. Scuseria, M.A. Robb, J.R. Cheeseman, V.G. Zakrzewski, J.A. Montgomery Jr., R.E. Stratmann, J.C. Burant, S. Dapprich, J.M. Millam, A.D. Daniels, K.N. Kudin, M.C. Strain, O. Farkus, J. Tomasi, V. Barone, M. Cossi, R. Cammi, B. Mennucci, C. Pomelli, C. Adamo, S. Clifford, J. Ochterski, G.A. Petersson, P.Y. Ayala, Q. Cui, K. Morokuma, D.K. Malick, A.D. Rabuck, K. Raghavachari, J.B. Foresman, J. Cioslowski, J.V. Ortiz, A.G. Baboul, B.B. Stefanov, G. Liu, A. Liashenko, P. Piskorz, I. Komaromi, R. Gomperts, R.L. Martin, D.J. Fox, T. Keith, M.A. Al-Laham, C.Y. Peng, A. Nanayakkara, M. Challacombe, P.M.W. Gill, B. Johnson, W. Chen, M.W. Wong, J.L. Andres, C. Gonzalez, M. Head-Gordon, E.S. Replogle, J.A. Pople, Gaussian Inc., Pittsburgh, PA, 1998.
[28] C. Gonzalez, H.B. Schlegel, J. Chem. Phys. 90 (1989) 2154.
[29] C. Gonzalez, H.B. Schlegel, J. Phys. Chem. 94 (1990) 5523.

[30] A.P. Scott, L. Radom, J. Phys. Chem. 100 (1996) 16502.
[31] T.H. Morton, Org. Mass Spectrom. 27 (1992) 353.
[32] D.J. McAdoo, T.H. Morton, Accts. Chem. Res. 26 (1993) 295.
[33] R. Postma, P.J.A. Ruttink, J.K. Terlouw, J.L. Holmes, J. Chem. Soc., Chem. Commun. (1986) 683.
[34] N. Heinrich, J. Schmidt, H. Schwarz, Y. Apeloig, J. Am. Chem. Soc. 109 (1987) 1317.
[35] T. Drewello, N. Heinrich, W.P.M. Maas, N.M.M. Nibbering, T. Weiske, H. Schwarz, J. Am. Chem. Soc. 109 (1987) 4810.
[36] N. Heinrich, H. Schwarz, Int. J. Mass Spectrom. Ion Processes 79 (1987) 295.
[37] R. Postma, P.J.A. Ruttink, J.H. Van Lenthe, J.K. Terlouw, Chem. Phys. Lett. 156 (1989) 245.
[38] W.J. Hehre, L. Radom, P.V.R. Schleyer, J.A. Pople, Ab Initio Molecular Orbital Theory, Wiley, New York, 1986, p. 25.
[39] T.H. Morton, Tetrahedron 38 (1982) 3195.
[40] W. Tumas, R.F. Foster, J.I. Brauman, J. Am. Chem. Soc. 106 (1984) 4053.
[41] P. Hobza, R. Zahradnik, Weak Intermolecular Interactions in Chemistry and Biology, Elsevier, New York, 1980, p. 139.
[42] K. Krogh-Jespersen, H.D. Roth, J. Am. Chem. Soc. 114 (1992) 8388.
[43] P. Longevialle, R. Botter, J. Chem. Soc., Chem. Commun. (1980) 823.
[44] C.E. Hudson, L. DeLeon, D. Van Alstyne, D.J. McAdoo, J. Am. Soc. Mass Spectrom. 5 (1994) 349.
[45] T. Baer, D. Smith, B.P. Tsai, A.S. Werner, Adv. Mass Spectrom. 7 (1977) 56.
[46] S.G. Lias, J.E. Bartmess, J.F. Liebman, J.L. Holmes, R.D. Levin, W.G. Mallard, J. Phys. Chem. Ref. Data 17 (1988).